Algebraic localization from power-law couplings in disordered quantum wires

Thomas Botzung,[1,2] Davide Vodola,[3,*] Piero Naldesi,[4,5] Markus Müller,[3] Elisa Ercolessi,[2,6] and Guido Pupillo[1,†]
[1]*University of Strasbourg, CNRS, ISIS (UMR 7006) and IPCMS (UMR 7504), 67000 Strasbourg, France*
[2]*Dipartimento di Fisica e Astronomia dell'Università di Bologna, I-40127 Bologna, Italy*
[3]*Department of Physics, Swansea University, Singleton Park, Swansea SA2 8PP, United Kingdom*
[4]*Université Grenoble-Alpes, LPMMC, F-38000 Grenoble, France*
[5]*CNRS, LPMMC, F-38000 Grenoble, France*
[6]*INFN, Sezione di Bologna, I-40127 Bologna, Italy*

(Received 24 October 2018; revised manuscript received 13 September 2019; published 22 October 2019)

We analyze the effects of disorder on the correlation functions of one-dimensional quantum models of fermions and spins with long-range interactions that decay with distance ℓ as a power law $1/\ell^{\alpha}$. Using a combination of analytical and numerical results, we demonstrate that power-law interactions imply a long-distance algebraic decay of correlations within disordered-localized phases, for all exponents α. The exponent of algebraic decay depends only on α, and not, e.g., on the strength of disorder. We find a similar algebraic localization for wave functions. These results are in contrast to expectations from short-range models and are of direct relevance for a variety of quantum mechanical systems in atomic, molecular, and solid-state physics.

DOI: 10.1103/PhysRevB.100.155136

I. INTRODUCTION

Quantum waves are generally localized exponentially by disorder. Following the seminal work by Anderson with spin-polarized electrons [1], much experimental [2–8] and theoretical interest has been devoted to the study of localized phases and to the localization-delocalization transition for noninteracting and interacting quantum models [9–30].

While most works have focused on short-range couplings, long-range hopping and interactions that decay with distance ℓ as a power law $1/\ell^{\alpha}$ have recently attracted significant interest [31–45] as they provide novel physical effects and can be now engineered in a variety of atomic, molecular, and optical systems. For example, the Ising model with power-law spin interactions with tunable exponent $0 < \alpha < 3$ has been first realized in breakthrough experiments with arrays of laser-driven cold ions [46–50] and could also be obtained with atoms trapped in a photonic crystal waveguide [51–54]; dipolar-type $1/\ell^3$ or van der Waals–type $1/\ell^6$ couplings have been recently demonstrated experimentally with ground-state neutral atoms [55–58], Rydberg atoms [59–73], polar molecules [74–76], and nuclear spins [77]. In solid-state materials, power-law hopping is of interest for, e.g., excitonic materials [78–90]; long-range $1/\ell$ coupling is found in helical Shiba chains [91,92], made of magnetic impurities on an *s*-wave superconductor, while planar arrays of Josephson Junctions [93,94] can effectively realize long-range extensions of the Kitaev chain for spinless fermions [95]. In the absence of disorder, theory and experiments have provided evidence for novel enticing static and dynamic phenomena in these systems, such as, e.g., the nonlocal propagation of correlations [33–35,96], time crystal phases [97], novel topological effects [98–103], and exotic behaviors of equal-time correlations, such as hybrid exponential and power-law decays within gapped phases, related to the violation of the area law for the entanglement entropy [104–107]. However, in many of these systems, disorder, in particles' positions, local energies, or coupling strengths, is an intrinsic feature. Understanding its effects on the above phenomena and in the context of single-particle and many-body localization remains a fundamental open question.

For noninteracting models, it is generally expected that long-range hopping induces delocalization in the presence of disorder for $\alpha < d$, while for $\alpha > d$ all wave functions are exponentially localized [1,108–114]. However, recent theoretical works with positional [115] and diagonal [114] disorder have demonstrated that localization can survive even for $\alpha < d$. Surprisingly, wave functions were found to be localized only algebraically in these models, in contrast to the usual Anderson-type exponential localization expected from short-range models. How these findings translate to the behavior of wave functions and, crucially, correlation functions in many-particle systems is not known.

In this work, we investigate the effects of disorder on the decay of correlation functions and wave functions in long-range quantum wires of fermions and spins. These are extensions of the Kitaev chain with long-range pairing [93,104,116] and the Ising model in a transverse field [117], providing both analytical insight and immediate experimental interest. While in the absence of disorder and for short-range interactions they are identical, for long-range interactions they correspond to integrable and nonintegrable chains, respectively. For fermions, we determine the regimes of localization for all α for the cases of disordered hopping or pairing. For the Ising chain, we focus on the regime $\alpha > 1$, where the disordered phase diagram has been shown to display many-body

*davide.vodola@gmail.com
†pupillo@unistra.fr

localization theoretically [118] and experimentally [7]. For all models we compute the one- and two-body connected correlation functions, finding several features: (i) The connected correlation functions decay algebraically at long distance within all localized phases, (ii) with an exponent that depends exclusively on α, and not, e.g., on the disorder strength. (iii) For the fermionic models, we derive analytic results for the long-distance decay of the correlations that explain the found algebraic decay, in excellent agreement with the numerics. (iv) The same analytical predictions are found to hold also for the correlations of the interacting Ising chain. (v) For any α, the localized wave functions of the fermionic models display a long-distance algebraic decay with exponent α, different from recent predictions for long-range hopping models. These results should be of direct relevance to many experiments in cold-atomic, molecular, and solid-state physics with fermions and spins.

II. MODELS

We consider the following Hamiltonians for one-dimensional long-range fermionic models

$$H_{\mathrm{I,II}} = H_0 + V_{\mathrm{I,II}}, \tag{1}$$

where H_0 is a homogeneous Hamiltonian given by

$$H_0 = -t\sum_{j=1}^{L}(a_j^\dagger a_{j+1} + \mathrm{H.c.}) + \mu\sum_{j=1}^{L} n_j + \sum_{j,\ell}\frac{\Delta}{\ell^\alpha}(a_j a_{j+\ell} + \mathrm{H.c.}) \tag{2}$$

that describes a p-wave superconductor with a long-range pairing, and the indices I, II refer to the two different types of Hamiltonians we consider, namely,

$$V_{\mathrm{I}} = \sum_{j=1}^{L} W_j(a_j^\dagger a_{j+1} + \mathrm{H.c.}) \tag{3}$$

that corresponds to a random hopping and

$$V_{\mathrm{II}} = \sum_{j,\ell}\frac{W_j}{\ell^\alpha}(a_j a_{j+\ell} + \mathrm{H.c.}) \tag{4}$$

that corresponds to a random long-range pairing. In the previous equations, $a_j^\dagger$ (a_j) is a fermionic creation (annihilation) operator on site j, μ is the chemical potential, $n_j = a_j^\dagger a_j$ and W_j are independent and identically distributed (i.i.d.) random variables drawn from a uniform distribution of width $2W$ and zero mean value. We fix the energy scale by letting $\Delta = 2t = 1$ and we choose $\mu = 2.5$, corresponding to a gapped paramagnetic phase [104] for $W_j = 0$. Different values of μ do not change the results we find in the following. The random Hamiltonians (1) can be written in diagonal form as $H_{\mathrm{I,II}} = \sum_{q=0}^{L-1}\Lambda_q\eta_q^\dagger\eta_q$ by a generalized Bogoliubov transformation [119] defined by $\eta_q = \sum_j(g_{q,j}a_j + h_{q,j}a_j^\dagger)$, with Λ_q the energies of the single-particle states labeled by q. The ground state $|\Omega\rangle$ is then the vacuum of all quasiparticles η_q and the matrix elements $g_{q,j}$ and $h_{q,j}$ can be identified with the wave functions of the two fermionic modes $\eta_q^\dagger$ and η_q, respectively.

As an interacting model, we consider the following random long-range Ising Hamiltonian [117] in transverse field:

$$H_{\mathrm{LRI}} = \sum_{j,\ell}(\sin\theta + B_{j,j+\ell})\frac{\sigma_j^x\sigma_{j+\ell}^x}{\ell^\alpha} + \sum_{j=1}^{L}(\cos\theta + W_j)\sigma_j^z, \tag{5}$$

where σ_j^ν ($\nu = x, z$) are Pauli matrices for a spin $\frac{1}{2}$ at site j and $B_{j,j+\ell}$ are i.i.d random variables drawn from a uniform distribution of width $2B$ and zero mean value. We choose $\theta = \pi/5$, corresponding to a paramagnetic phase [116] for $B_{j,j+\ell} = W_j = 0$. Different values of θ will not change the results we find in the following. For any finite disorder strength, the model (5) displays a many-body localized (MBL) phase [120–124] for $\alpha > 1$.

In the following, we first determine the regimes of localization for the fermionic models (1) and then compute the single- and the two-body correlation functions, as well as the wave functions, within the localized phases using analytical and numerical techniques. For the long-range Ising model (5) we compute the spin-spin connected correlation functions numerically. Our goal is to demonstrate that all these quantities decay algebraically at large distances both for noninteracting and interacting MBL localized models and to characterize their decay exponents.

III. LOCALIZED PHASES OF DISORDERED FERMIONS

We determine the localized phases for Hamiltonians (1) by combining information from the inverse participation ratio (IPR). The IPR gives information about the spatial extension of single-particle states and is defined as $\mathrm{IPR}_q = \sum_{j=1}^{L}[|g_{q,j}|^4 + |h_{q,j}|^4]$ for a normalized state with energy Λ_q. The IPR tends to zero for increasing L for extended states, while it remains finite for localized states.

Figure 1 shows the IPR as a function of W for all the single-particle eigenstates of a system of $L = 1000$ for model (1), I [for $\alpha = 3$ and 0.8 in Figs. 1(a) and 1(b), respectively] and II [for $\alpha = 3$ in Fig. 1(c)] together with examples of finite-size scaling [Figs. 1(d) and 1(e)].

For model I with disordered hopping and $\alpha > 1$ [Fig. 1(a)] essentially all states are localized. For $\alpha < 1$ [Fig. 1(b)] we find that, at W fixed, there exists an energy below (above) which all the states are localized (delocalized). However, the fraction of delocalized states that are found at high energy scales to zero as $\sim 1/L^{1/(4-2\alpha)}$ and those states approach the band edge for $L \to \infty$ (see Appendix B). For model II with disordered pairing when $\alpha > 1$ localized states are present at all energies if $W \gtrsim 2$ [Fig. 1(c)].

IV. CORRELATION FUNCTIONS

We consider the single-particle correlator $C(j,\ell) = \langle a_j^\dagger a_{j+\ell}\rangle_W$ for the two free-fermionic models of Eqs. (1) as well as the spin-spin correlation function $S_\nu(j,\ell) = [\langle\sigma_j^\nu\sigma_{j+\ell}^\nu\rangle - \langle\sigma_j^\nu\rangle\langle\sigma_{j+\ell}^\nu\rangle]_W$ (for $\nu = x, z$) for the interacting long-range Ising model of Eq. (5) in the localized phases. In the definitions of $C(j,\ell)$ and $S_\nu(j,\ell)$ the subscript W

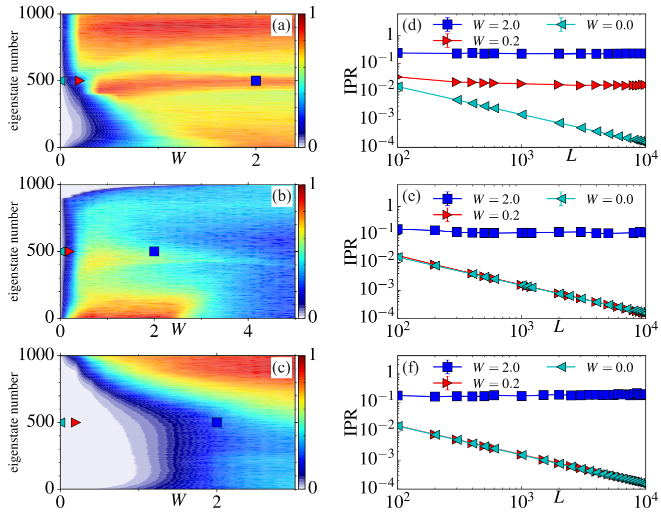

FIG. 1. Left panels: IPR for a system of $L = 1000$ sites as a function of the disorder strength W for (a) $\alpha = 3$ and (b) $\alpha = 0.8$ for the model I with random hopping and (c) for $\alpha = 3.0$ for the model II with random pairing. Only in these panels, for drawing purpose, the IPR has been rescaled to 1 in correspondence of its maximum value. Right panels: scaling of the IPR for the states at the center of the band as a function of the system size L and different W for (d) $\alpha = 3$ and (e) $\alpha = 0.8$ for the model I and (f) for $\alpha = 3.0$ for the model II. In (a)–(c) the symbols indicate the values of W that we choose to plot the IPR in (d)–(f).

indicates averaging over the disorder distribution. For models with short-range interactions, all the correlation functions decay exponentially with ℓ. For models with-long range coupling, it has been shown that correlation functions can display a power tail at long distance (see Appendix A). Here, we are interested in the effects that can originate from the interplay between long-range interactions and disorder.

Figures 2(a) and 2(b) show the correlator $C(\ell) := C(j_0, \ell)$ for models $H_{\rm I}$ and $H_{\rm II}$, respectively, for different values of α. We choose $j_0 = L/4$ far from the edges in order to avoid boundary effects. We find numerically that the long-distance decay of $C(\ell)$ is always of power-law type $C(\ell) \sim \ell^{-\gamma}$ for all α within localized phases. In particular, for model $H_{\rm I}$ [Fig. 2(a)] and $\alpha < 1$ the decay is essentially algebraic at all distances with $\gamma \sim 2 - \alpha$, while for $\alpha > 1$ we find for both models a hybrid decay that is exponential at short distances and power law at large distances, with $\gamma \sim \alpha$ [Figs. 2(a)

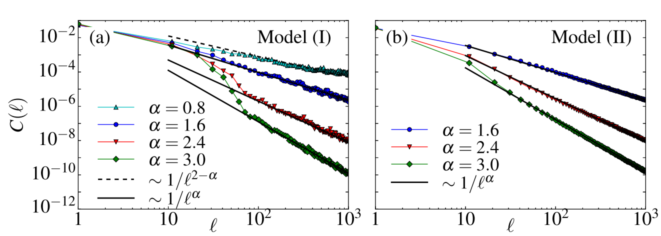

FIG. 2. (a) Correlation function $C(\ell)$ for the model I as a function of the lattice site ℓ for different values of α and for $W = 5$, $L = 2000$ and 400 disorder realizations. The power-law tails are fit by the black lines scaling as $1/\ell^{2-\alpha}$ (dashed) and $1/\ell^{\alpha}$ (solid) in agreement with the analytical results in Eq. (11). (b) Same as (a) but for the model II.

and 2(b)]. Surprisingly, we find that the values of the decay exponents of the power-law tails do not depend on the disorder strength (see Appendix C). Remarkably, we observe that this behavior is typical also of states far from the bottom of the energy band. This is shown in Appendix C, where we compute the one-body correlation function of a localized single-particle state at the center of the energy band. This is reminiscent of recent results for fermions at finite temperature, in the absence of disorder [43].

This surprising long-distance behavior of correlations can be understood by computing the correlations analytically treating disorder as a perturbation. Here, we focus on model I with perturbation $V_{\rm I}$. The homogeneous Hamiltonian H_0 can be diagonalized via Fourier and Bogoliubov transformations as $H_0 = \sum_k \lambda_\alpha(k) \xi_k^\dagger \xi_k$, where $\lambda_\alpha(k) = [(\cos k - \mu)^2 + 4 f_\alpha^2(k)]^{1/2}$ and ξ_k are extended Bogolioubov quasiparticles related to the unperturbed fermionic operators in momentum space via $\tilde{a}_k = v_k \xi_k - u_k \xi_{-k}^\dagger$ with $v_k = \cos\varphi(k)$ and $u_k = i \sin\varphi(k)$, with $\tan 2\varphi(k) = f_\alpha(k)/[\mu - \cos k]$ and $f_\alpha(k) = \sum_{\ell=1}^{L-1} \sin(k\ell)/\ell^\alpha$. At first order in W_j the ground state $|\Omega_0\rangle$ of the unperturbed Hamiltonian H_0 is modified by $V_{\rm I}$ as

$$|\Omega\rangle = |\Omega_0\rangle + |\delta\Omega_0\rangle = |\Omega_0\rangle - \sum_{kk'} J_{k,k'} A(k,k') \xi_k^\dagger \xi_{k'}^\dagger |\Omega_0\rangle , \tag{6}$$

where we define $J_{k,k'} = -\sum_j e^{i(k-k')j} W_j/L$ and $A(k,k') = 2(e^{ik} + e^{-ik'}) v_k u_{k'}^* / [\lambda(k) + \lambda(k')]$. We find that $\langle\Omega|H|\Omega\rangle$ provides an excellent approximation of the exact ground-state energy for $0 < W < 3$ (see Appendix C), suggesting that $|\Omega\rangle$ is a good approximate ground state in that range. For correlations, since $\langle J_{k,k'}\rangle_W = 0$, we find that $\langle\delta\Omega_0|a_j^\dagger a_{j+\ell}|\Omega_0\rangle_W$ and $\langle\Omega_0|a_j^\dagger a_{j+\ell}|\delta\Omega_0\rangle_W$ vanish due to averaging over the disorder distribution. We obtain the following expression for $C(\ell)$:

$$\langle\Omega|a_j^\dagger a_{j+\ell}|\Omega\rangle_W = \langle\Omega_0|a_j^\dagger a_{j+\ell}|\Omega_0\rangle + \langle\delta\Omega_0|a_j^\dagger a_{j+\ell}|\delta\Omega_0\rangle_W . \tag{7}$$

The first term in the right-hand side of Eq. (7) corresponds to the correlator of the homogeneous system [116] that is $\langle\Omega_0|a_j^\dagger a_{j+\ell}|\Omega_0\rangle = \int_0^{2\pi} dk\, e^{ik\ell} R_0(k)$, with $R_0(k) = |u_k|^2$. The second term arises instead because of the random part of the Hamiltonian and reads as

$$\langle\delta\Omega_0|a_j^\dagger a_{j+\ell}|\delta\Omega_0\rangle_W = \frac{2W^2}{3} \int_0^{2\pi} dk\, e^{ik\ell} R_1(k), \tag{8}$$

where we have defined $R_1(k) = [c - U(k)]|u_k|^2 - V(k)|v_k|^2$, with c that does not depend on k, $V(k) = \sum_p A(p,k)A(k,p) \sim f_\alpha(k)/\lambda_\alpha(k)$ and $U(k) = V(-k)$. The behavior of both integrals for $\ell \to \infty$ can be extracted by integrating $R_0(k)$ and $R_1(k)$ for $k \to 0$. In this limit $f_\alpha(k)$, and thus the single-particle energy $\lambda_\alpha(k)$, display a nonanalytical scaling $f_\alpha(k) \sim |k|^{\alpha-1}$. For the first term in the right-hand side of Eq. (7) the latter behavior results in (details in Appendix C)

$$\langle\Omega_0|a_j^\dagger a_{j+\ell}|\Omega_0\rangle \sim \begin{cases} 1/\ell^{2-\alpha} & \text{for } \alpha < 1, \\ 1/\ell^{2\alpha-1} & \text{for } 1 < \alpha < 2, \\ 1/\ell^{\alpha+1} & \text{for } \alpha > 2, \end{cases} \tag{9}$$

which corresponds to the expected long-distance power-law decay of correlation functions for the homogeneous gapped

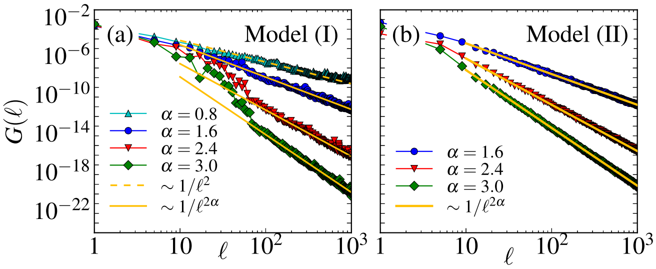

FIG. 3. (a) Density-density correlation function $G(\ell)$ for the model I as a function of the lattice site ℓ for different values of α and for $W = 5$, $L = 2000$ and 400 disorder realizations. The power-law tails are fit by the yellow lines scaling as $1/\ell^2$ (dashed) and $1/\ell^{2\alpha}$ (solid). (b) Same as (a) but for the model II.

superconductor with long-range pairing [104,116,125–127]. Instead, for $R_1(k)$ the scaling of $f_\alpha(k)$ near $k \to 0$ implies

$$R_1(k) \sim \begin{cases} k^{1-\alpha} & \text{for } \alpha < 1, \\ k^{\alpha-1} & \text{for } \alpha > 1, \end{cases} \tag{10}$$

which entails the following form of the disordered part of $C(\ell)$:

$$\langle \delta\Omega_0 | a_j^\dagger a_{j+\ell} | \delta\Omega_0 \rangle_W \sim \begin{cases} W^2/\ell^{2-\alpha} & \text{for } \alpha < 1, \\ W^2/\ell^{\alpha} & \text{for } \alpha > 1 \end{cases} \tag{11}$$

after the integration of $R_1(k)$ in Eq. (8)

The discussion above demonstrates the following surprising results: (i) For $\alpha < 1$, disorder does not modify the power of the algebraic decay of correlations, rather it affects its strength. (ii) For $\alpha > 1$, the decay of correlations due to disorder is always algebraic, with an exponent that is smaller than for the homogeneous case with $W_j = 0$. This implies that disorder enhances algebraic localization in these gapped models. (iii) For $\alpha \leqslant 2$, we find the duality relation $\gamma(\alpha) = \gamma(2 - \alpha)$ in the exponents of the algebraic decay. This is reminiscent of the duality recently found for the decay exponent of the wave functions of long-range noninteracting spin models with positional disorder [115]. We come back to this point below.

From the single-particle correlators $\langle a_j^\dagger a_{j+\ell} \rangle$ and $\langle a_j^\dagger a_{j+\ell}^\dagger \rangle$, by means of the Wick theorem, we computed also the density-density correlation functions

$$\begin{aligned} G(j,\ell) &= [\langle n_j n_{j+\ell} \rangle - \langle n_j \rangle \langle n_{j+\ell} \rangle]_W \\ &= [|\langle a_j a_{j+\ell} \rangle|^2 - |\langle a_j^\dagger a_{j+\ell} \rangle|^2]_W. \end{aligned} \tag{12}$$

Examples of $G(\ell) = G(j_0, \ell)$ with $j_0 = L/4$ are shown in Fig. 3 for a system of $L = 2000$ sites and for a disorder strength $W = 5$. Numerically, we find that in the localized phases for model (I) when $\alpha < 1$, $G(\ell) \sim 1/\ell^2$ while for both models $G(\ell) \sim 1/\ell^{2\alpha}$ when $\alpha > 1$. The first behavior with a decay exponent that does not depend on α has been already observed in Refs. [104,116], while the second can be explained by looking at the $\ell \to \infty$ scaling of $|C(\ell)|^2 \sim 1/\ell^{2\alpha}$ in Eq. (C26) in Appendix C.

For the random interacting long-range Ising model, we compute the spin-spin correlation functions $S_\nu(\ell) := S_\nu(j_0, \ell)$ ($\nu = x, z$) within the MBL phase with $\alpha > 1$, by using a density matrix renormalization group (DMRG) algorithm [128].

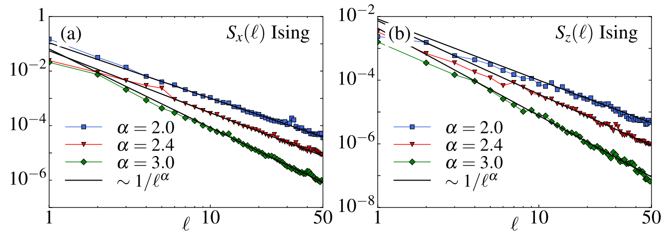

FIG. 4. (a) Correlation function $S_x(\ell)$ for the long-range Ising model with a random transverse field [$W = 5\sin(\pi/5)$] and a constant interaction term ($B = 0$) for a system of $L = 100$ spins and 50 disorder realizations. (b) Correlation function $S_z(\ell)$ for the long-range Ising model with a random interaction [$B = 5\sin(\pi/5)$] and a constant magnetic field ($W = 0$). In both panels, the power-law tails are fit by the black lines scaling as $1/\ell^{\alpha}$.

Here we choose $j_0 = L/10$. For the simulations, we use up to 400 local DMRG states, 16 sweeps, and we average $S_\nu(\ell)$ over 100 disorder realizations. Strikingly, we find that $S_\nu(\ell)$ decays algebraically with ℓ as $S_\nu(\ell) \sim \ell^{-\gamma}$ with an exponent that is consistent with $\gamma = \alpha$, in complete agreement with the discussion above for noninteracting theories. As an example, Fig. 4(a) shows $S_x(\ell)$ for different values of α, $W = 5\sin(\pi/5) \approx 2.93$, and $B = 0$, while Fig. 4(b) shows $S_z(\ell)$ for different values of α, $W = 0$, and $B = 5\sin(\pi/5)$. The corresponding fits (continuous lines) with $1/\ell^{\alpha}$ perfectly match the numerical results.

The demonstration of algebraic localization found in long-range couplings in the presence of disorder is a central result of this work. We argue that the fact that these results are found both for noninteracting and interacting models strongly suggests the existence of a universal behavior due to long-range coupling.

V. LOCALIZATION OF WAVE FUNCTIONS

Numerical results on the decay of the single-particle wave functions are obtained by considering the mean value $\Phi(\ell) = \sum_{q=1}^{N} |g_{q,\ell-j_M}|/N$ where we average $N = L/4$ wave functions $g_{q,\ell}$ with lowest energies, shifted by the quantity j_M that corresponds to the lattice site where $|g_{q,\ell}|$ shows its maximum value. We average $\Phi(\ell)$ also over several disorder realizations (of the order of 500).

Figure 5 shows typical results of the decay of $\Phi(\ell)$ as a function of the distance ℓ within the localized phases of models I and II of Eqs. (1) [Figs. 5(a) and 5(b) and 5(c) and 5(d), respectively].

Remarkably, we find that the wave functions decay algebraically at long distances regardless of the strength W of the disorder, mimicking the scaling of the correlation functions discussed above. However, for all α, i.e., both $\alpha > 1$ and $\alpha < 1$, $\Phi(\ell)$ decays at large distances as $\Phi(\ell) \sim \ell^{-\gamma_{\rm wf}}$, with an exponent $\gamma_{\rm wf}$ consistent with $\gamma_{\rm wf} \sim \alpha$. This is different from the results of Ref. [115] with positional disorder, where for $\alpha < 1$ one gets $\gamma_{\rm wf} \sim 2 - \alpha$. For sufficiently large $\alpha > 1$ this algebraic decay is preceded by an exponential decay at short distances, reminiscent of the exponentially localized states of short-range random Hamiltonians.

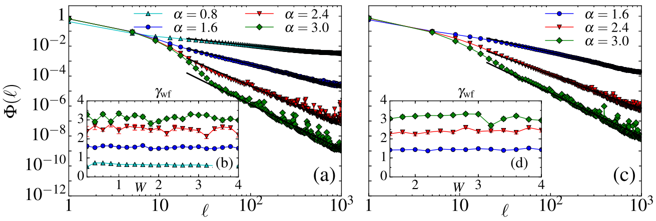

FIG. 5. (a) Decay of the averaged wave function $\Phi(\ell)$ (absolute value, see text) of localized states for the model I: If $\alpha > 1$ we find a hybrid exponential and power-law behavior. If $\alpha < 1$ the exponential part is suppressed and only the power-law tail is visible. The black lines correspond to fit of the data scaling as $1/\ell^{\gamma_{\rm wf}}$. (b) Decay exponent $\gamma_{\rm wf}$ for the model I of the long-distance tail of $\Phi(\ell)$ as a function of W for different values of α. The decay exponent satisfies $\gamma_{\rm wf} \sim \alpha$ and does not show significance dependence on W. (c), (d) Same as (a) and (b) but for the model II with random long-range pairing.

VI. CONCLUSIONS

In this work we have demonstrated that couplings that decay as a power law with distance induce an algebraic decay of correlation functions and wave functions both in noninteracting and interacting models in the presence of disorder. This is in stark contrast to results expected from short-range models, and generalizes recent results for the decay of wave functions in quadratic models. These results are of immediate interest for experiments with cold ions, molecule, Rydberg atoms, and quantum emitters in cavity fields, to name a few. It is an exciting prospect to explore the properties of many-body quantum phases in the search of exotic transport phenomena with long-range interactions.

ACKNOWLEDGMENTS

P.N. thanks L. Benini for fruitful discussions. G.P. acknowledges support from ANR "ERA-NET QuantERA"-Projet "RouTe" and UdS via Labex NIE. G.P. acknowledges additional support from the Institut Universitaire de France (IUF) and the University of Strasbourg Institute for Advanced Studies (USIAS). E.E. is partially supported through the project "QUANTUM" by Istituto Nazionale di Fisica Nucleare (INFN) and through the project "ALMAIDEA" by University of Bologna. The DMRG simulations were performed using the ITensor library [129].

APPENDIX A: CORRELATION IN THE LONG-RANGE MODELS WITH NO DISORDER

In this Appendix we summarize some results on the decay of the correlation functions for both the long-range Kitaev and Ising models in the absence of disorder. For the long-range Kitaev model, it has been shown in Refs. [104,116,125] that the one-body correlation function $C(j,\ell) = \langle a_j^\dagger a_\ell \rangle$ shows a different behavior depending on the value α of the decay exponent of the pairing term. In the limit of a infinite system the one-body correlator takes the form of an integral on the Brillouin zone:

$$C(j,\ell) = \langle a_j^\dagger a_\ell \rangle = \frac{1}{2\pi}\int_0^{2\pi} dk\, \frac{\mu + \cos k}{\lambda_\alpha(k)} e^{ik(j-\ell)}, \qquad \text{(A1)}$$

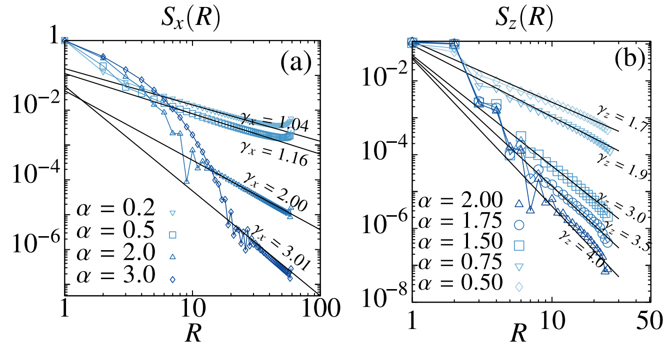

FIG. 6. (a) $S_x(R)$ correlation for the long-range Ising model [Eq. (5) of the main text] for $B_{ij} = W_{ij} = 0$ ($\theta = 0.2\pi$ and $L = 60$), showing the hybrid exponential and power-law behavior for $\alpha \gtrsim 1$ and a purely power law for $\alpha \lesssim 1$. (b) $S_z(R)$ correlation for the long-range Ising model [Eq. (5) of the main text] for $B_{ij} = W_j = 0$ and $\theta = 0.207\pi$, $L = 100$, and different α.

where $\lambda_\alpha(k) = [(\cos k - \mu)^2 + 4 f_\alpha^2(k)]^{1/2}$ and $f_\alpha(k) = \mathrm{Im}\,\mathrm{Li}_\alpha(e^{ik})$. An explicit calculation of the previous integral gives

$$C(R) \equiv C(R,0) \sim e^{-\xi R} + A(\alpha,\mu)\cdot \begin{cases} \frac{1}{R^{\alpha+1}} & \text{if } \alpha > 2; \\ \frac{1}{R^{2\alpha-1}} & \text{if } 1 < \alpha < 2; \\ \frac{1}{R^{2-\alpha}} & \text{if } 0 < \alpha < 1. \end{cases} \qquad \text{(A2)}$$

The parameter ξ is the smallest real solution of $\lambda_\alpha(i\pi + \xi) = 0$ and depends on μ and α in an implicit way and the coefficient $A(\alpha,\mu)$ can be found in Ref. [125]. It is possible to see that the correlation function shows a hybrid decay, i.e., exponential at short distances, followed by an algebraic tail whose decaying exponent depends on α.

For the long-range Ising model, Ref. [116] showed that the connected part of the correlation functions

$$S_\nu(j,\ell) = \langle \sigma_j^\nu \sigma_{j+\ell}^\nu \rangle - \langle \sigma_j^\nu \rangle \langle \sigma_{j+\ell}^\nu \rangle, \qquad \text{(A3)}$$

for $\nu = x, z$, decay with distance with a hybrid behavior that is exponential at short distances and algebraic at long ones.

An example is shown in Fig. 6(a) for $S_x(R) \equiv S_x(R,0)$. The exponent γ_x of the long-distance decay displays three difference behaviors: (i) For $\alpha > 2$ it fulfills $\gamma_x = \alpha$. (ii) For $1 < \alpha < 2$, a hybrid decay is observed and the algebraic tail decays with an exponent γ that depends linearly on α with a slope consistent with $\sim$0.55. (iii) For $\alpha \lesssim 1$, $\gamma_x \sim 0.25\alpha$. The correlator $S_z(R)$ is shown in Fig. 6(b) and it also displays an algebraic tails that decays as $1/R^{\gamma_z}$ where $\gamma_z \sim 2\alpha$ for $\alpha > 1$.

APPENDIX B: ENERGY SCALING ANALYSIS

In this Appendix we give an analytical insight (based essentially on Ref. [112]) on the different behaviors of the IPR [plotted in Figs. 1(a) and 1(b) of the main text] of the single-particle states for the Hamiltonians I when $\alpha > 1$ and $\alpha < 1$.

For the Hamiltonian I, the random term $V_{\rm I}$, which reads as $V_{\rm I} = \sum_{kk'} J_{k,k'} (e^{ik} + e^{-ik'}) a_k^\dagger a_{k'}$ with $J_{k,k'} = -\sum_j e^{i(k-k')j} W_j / L$ after a Fourier transform, couples the extended eigenmodes of H_0 to each others and it can lead to localization if the mean fluctuation $\sigma_{\rm I}^2 := \langle J_{k,k'}^2 \rangle = \delta_{kk'} W^2/(3L)$ is much larger than the level spacing $\delta\lambda_\alpha$ of the energies $\lambda_\alpha(k)$ of H_0. Here, we will restrict our attention to those states lying either at the minimum or at the maximum of $\lambda_\alpha(k)$. The level spacing $\delta\lambda_\alpha$ can be computed analytically from $\lambda_\alpha(k)$ and it strongly depends on α: (i) If $\alpha > 1$, $\lambda_\alpha(k)$ is finite for all k and we obtain $\lambda_\alpha(k) \sim k^2$ both at the minimum and at the maximum of the band. The corresponding level spacing thus scales with L as $\delta\lambda_{\alpha>1} \sim 1/L^2$ and it decays faster than $\sigma_{\rm I}$. In this case, the extended states of H_0 are coupled by the random part of $V_{\rm I}$ and they will be localized. No mobility edge is then expected for $\alpha > 1$. The IPR computed for this case is shown in Fig. 1(a).

On the contrary, (ii) if $\alpha < 1$ the energy diverges as $\lambda_\alpha(k) \sim 1/|k|^{1-\alpha}$ and the level spacing for the high-energy states grows as $\delta\lambda_{\alpha<1} \sim L^{1-\alpha}$. The fluctuation of the random couplings $\sigma_{\rm I} \sim 1/\sqrt{L}$ is thus suppressed by $\delta\lambda_{\alpha<1}$ and the high-energy states of H_0 remain extended. As the lowest-energy states can be localized, a single-particle mobility edge can be then expected for all $\alpha < 1$. By the equality $\delta\lambda_{\alpha<1} \sim \sigma_{\rm I}$ that defines the single-particle mobility edge, it is possible to show that the number of extended states increases with L as $N_{\rm ext} \sim L^{(3/2-\alpha)/(2-\alpha)}$ but their fraction $N_{\rm ext}/L$ vanishes in the thermodynamic limit [113]. The IPR for this case is shown in Fig. 1(b).

APPENDIX C: DECAY OF CORRELATION FUNCTIONS

In this Appendix we show how to compute the correlation function $C(j,i) = \langle a_j^\dagger a_i \rangle$ of the model with random hopping by perturbation theory.

1. Correlation functions: Perturbation theory

We recall that the Hamiltonian $H_{\rm I}$ in Eq. (1) is formed by two parts:

$$H_{\rm I} = H_0 + V_{\rm I}. \tag{C1}$$

In order to compute the correlation function $C(j,i) = \langle\Omega|a_j^\dagger a_i|\Omega\rangle$ on the ground state $|\Omega\rangle$ of $H_{\rm I}$ in Eq. (1), we first find the first-order correction $|\delta\Omega_0\rangle$ to the ground state $|\Omega_0\rangle$ of H_0 by treating $V_{\rm I}$ as a perturbation.

The first-order correction $|\delta\Omega_0\rangle$ to the ground state $|\Omega_0\rangle$ of the Hamiltonian H_0 due to the perturbation $V_{\rm I}$ is given by [130]

$$|\delta\Omega_0\rangle = \sum_{\mathbf{n}_0} \frac{\langle \mathbf{n}_0|V_{\rm I}|\Omega_0\rangle}{E(\mathbf{n}_0) - E_0} |\mathbf{n}_0\rangle\,, \tag{C2}$$

where the quantities $E(\mathbf{n}_0)$ and E_0 are the energy of the states $|\mathbf{n}_0\rangle$ and of $|\Omega_0\rangle$, respectively, and $|\mathbf{n}_0\rangle$ indicates an excited state of the homogeneous Hamiltonian H_0 that can be diagonalized via Fourier and Bogoliubov transformations as

$$H_0 = \sum_k \lambda_\alpha(k) \xi_k^\dagger \xi_k. \tag{C3}$$

The ground state $|\Omega_0\rangle$ of H_0 is then the vacuum of all quasiparticles ξ_k.

In Eq. (C3) we have defined the single-particle energy

$$\lambda_\alpha(k) = [(\cos k - \mu)^2 + 4 f_\alpha^2(k)]^{1/2} \tag{C4}$$

and the Bogolioubov quasiparticles ξ_k that are related to the original fermionic operators $\tilde{a}_k$ in momentum space via

$$\tilde{a}_k = v_k \xi_k - u_k \xi_{-k}^\dagger \tag{C5}$$

with $v_k = \cos\varphi(k)$ and $u_k = i\sin\varphi(k)$ where $\tan 2\varphi(k) = f_\alpha(k)/[\mu - \cos k]$ and $f_\alpha(k) = \sum_{\ell=1}^{L-1} \sin(k\ell)/\ell^\alpha$. We notice that the functions $f_\alpha(k)$ when $L\to\infty$ become $f_\alpha(k) = [\mathrm{Li}_\alpha(e^{ik}) - \mathrm{Li}_\alpha(e^{-ik})]/(2i)$, with $\mathrm{Li}_\alpha(z) = \sum_j z^j/j^\alpha$ a polylogarithm of order α.

The excited states $|\mathbf{n}_0\rangle$ are defined by assigning a set of occupied modes $\mathbf{n}_0 = \{n_1, n_2, \ldots, n_L\}$ with $n_q = 0, 1$ and then creating single quasiparticles $\xi_q^\dagger$ on the ground state $|\Omega_0\rangle$ if the mode q is occupied:

$$|\mathbf{n}_0\rangle = \prod_{q=0}^{L-1} [\xi_q^\dagger]^{n_q} |\Omega_0\rangle\,. \tag{C6}$$

The first-order correction $|\delta\Omega_0\rangle$ can now be obtained from Eq. (C2) and the true ground state $|\Omega\rangle$ becomes

$$\begin{aligned}|\Omega\rangle &= |\widetilde{\Omega}\rangle + \mathcal{O}(W^2)\\ &= |\Omega_0\rangle + |\delta\Omega_0\rangle + \mathcal{O}(W^2)\\ &= |\Omega_0\rangle - \sum_{kk'} J_{k,k'} A(k,k') \xi_k^\dagger \xi_{k'}^\dagger |\Omega_0\rangle + \mathcal{O}(W^2),\end{aligned} \tag{C7}$$

where we have defined $J_{k,k'} = -\sum_j e^{i(k-k')j} W_j/L$ and $A(k,k') = 2(e^{ik} + e^{-ik'}) v_k u_{k'}^*/[\lambda(k) + \lambda(k')]$.

On a single disorder realization the correlation function $\langle\Omega|a_j^\dagger a_i|\Omega\rangle$ takes the form

$$\begin{aligned}\langle\Omega|a_j^\dagger a_i|\Omega\rangle &= \langle\Omega_0|a_j^\dagger a_i|\Omega_0\rangle + \langle\delta\Omega_0|a_j^\dagger a_i|\Omega_0\rangle\\ &\quad + \langle\Omega_0|a_j^\dagger a_i|\delta\Omega_0\rangle + \langle\delta\Omega_0|a_j^\dagger a_i|\delta\Omega_0\rangle\,.\end{aligned} \tag{C8}$$

If we now average Eq. (C8) over many disorder realizations, the cross terms $\langle\delta\Omega_0|a_j^\dagger a_i|\Omega_0\rangle$ and $\langle\Omega_0|a_j^\dagger a_i|\delta\Omega_0\rangle$ vanish as, due to the correction $|\delta\Omega_0\rangle$, only one random term W_j (that has mean value zero) appears in them. Therefore, we get

$$\langle\Omega|a_j^\dagger a_i|\Omega\rangle_W = \langle\Omega_0|a_j^\dagger a_i|\Omega_0\rangle + \langle\delta\Omega_0|a_j^\dagger a_i|\delta\Omega_0\rangle_W\,. \tag{C9}$$

The first term of the right-hand side of Eq. (C9) corresponds to the correlator for a homogeneous translationally invariant system. By rewriting $a_j^\dagger$ and a_i in momentum space and by using Eq. (C5) recalling that $\xi_k|\Omega_0\rangle = 0$ we obtain

$$C_0(\ell) := \langle\Omega_0|a_j^\dagger a_i|\Omega_0\rangle = \frac{1}{L}\sum_k e^{ik\ell} R_0(k), \tag{C10}$$

where $\ell = j - i$ and $R_0(k) = |u_k|^2$.

In the second term of the right-hand side of Eq. (C9), as we are averaging on the disorder configurations, we can expect that the disorder average $\langle\delta\Omega_0|a_j^\dagger a_i|\delta\Omega_0\rangle_W$ will be translationally invariant, i.e., it will depend on the relative distance $\ell = j - i$ while the terms that depend on i and j separately will average out to zero (see Sec. 6.5 in Ref. [131] or Sec. 12.3 in Ref. [132]). By keeping only the terms that depend on ℓ, after rewriting $a_j^\dagger$ and a_i in momentum space and using again Eq. (C5) recalling that $\xi_k\,|\Omega_0\rangle = 0$, the second term becomes

$$C_1(\ell) := \langle\delta\Omega_0|a_j^\dagger a_i|\delta\Omega_0\rangle_W = \frac{W^2}{3L}\sum_k e^{ik\ell}R_1(k), \tag{C11}$$

where

$$R_1(k) = c|u_k|^2 + U(k)|u_k|^2 - V(k)|v_k|^2, \tag{C12}$$

$$c = \sum_p A(p,p)^2 - \sum_{p_1p_2} A(p_1,p_2)A(p_2,p_1), \tag{C13}$$

$$\begin{aligned} U(k) &= 2\sum_p A(p,-k)A(-k,p) \\ &= -\frac{f_\alpha(k)}{\lambda_\alpha(k)}\sum_p \frac{2+2\cos(p-k)}{(\lambda_\alpha(k)+\lambda_\alpha(p))^2}\frac{f_\alpha(p)}{\lambda_\alpha(p)}, \end{aligned} \tag{C14}$$

$$V(k) = U(-k). \tag{C15}$$

We note that the quantity c does not depend on k.

2. Correlation functions: Asymptotic behavior

In this section we show how the two correlators $C_0(\ell)$ and $C_1(\ell)$ behave asymptotically for $\ell \to \infty$. Let us consider $C_0(\ell)$ in Eq. (C10) first. In the limit $L \to \infty$ we can replace the summation with an integral

$$C_0(\ell) = \frac{1}{2\pi}\int_{-\infty}^{\infty} dk\, e^{ik\ell}R_0(k). \tag{C16}$$

The asymptotic behavior of $C_0(\ell)$ for $\ell \to \infty$ can be computed by considering the integrals I_0^+ and I_0^- on the complex plane in Fig. 7 that are

$$\begin{aligned} I_0^\pm &= \frac{1}{2\pi}\int_{s_\pm} dz\, e^{iz\ell}R_0(z) + \frac{1}{2\pi}\int_{\Gamma_\pm} dz\, e^{iz\ell}R_0(z) \\ &\quad + \frac{1}{2\pi}\int_0^{\infty} dk\, e^{ik\ell}R_0(k), \end{aligned} \tag{C17}$$

where we have chosen to put the branch cut of the complex logarithm [see the expansion of the polylogarithm in Eq. (C19)] on the imaginary positive axis.

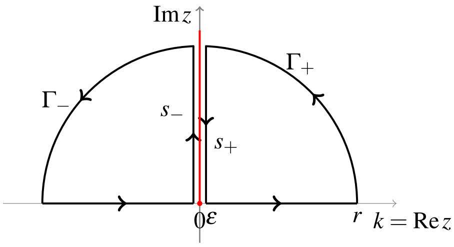

FIG. 7. Integration contour for evaluating the asymptotic behaviors of the correlators $C_0(\ell)$ in Eq. (C18) and $C_1(\ell)$ in Eq. (C23).

By sending the radius r of the circles $\Gamma_\pm$ to infinity and by neglecting possible residues inside the integration contour that will contribute only with exponential decaying terms, we have

$$\begin{aligned} C_0(\ell) &= -\frac{1}{2\pi}\int_{s_+} dz\, e^{iz\ell}R_0(z) - \frac{1}{2\pi}\int_{s_-} dz\, e^{iz\ell}R_0(z) \\ &= \frac{i}{2\pi}\int_0^{\infty} dy\, e^{-y\ell}R_0(\epsilon+iy) \\ &\quad - \frac{i}{2\pi}\int_{-\infty}^{0} dy\, e^{-y\ell}R_0(-\epsilon+iy) \\ &= \frac{1}{\pi}\int_0^{\infty} dy\, e^{-y\ell}\,\mathrm{Im}\,R_0(iy), \end{aligned} \tag{C18}$$

where on the lines $s_\pm$ the complex variable is $z = \pm\epsilon + iy$ with ϵ a small positive parameter that we send to zero.

We are able now to evaluate the asymptotic behavior of $C_0(\ell)$ by computing the $y \to 0$ part of $\mathrm{Im}[R_0(iy)]$ and then integrating the last equality in Eq. (C18). This is done by recalling that the polylogarithm admits the series expansion [133,134] for a general complex number z as

$$\mathrm{Li}_\alpha(z) = \Gamma(1-\alpha)\left(\ln\frac{1}{z}\right)^{\alpha-1} + \sum_{n=0}^{\infty}\zeta(\alpha-n)\frac{(\ln z)^n}{n!} \tag{C19}$$

that makes them nonanalytical due to the presence of the complex logarithm and the power law. In Eq. (C19), $\Gamma(x)$ and $\zeta(x)$ are the Euler gamma function and the Riemann zeta function, respectively.

By using the series expansion of the polylogarithms from Eq. (C19) we can obtain the function $R_0(iy)$ on the imaginary axis:

$$R_0(iy) = \frac{\mu-\cosh y}{2\lambda_\alpha(iy)} \sim \frac{\mu-1}{2\sqrt{(\mu-1)^2 - \Gamma^2(1-\alpha)(e^{i\pi\alpha}+1)^2y^{2\alpha-2} - 4\Gamma(1-\alpha)(e^{i\pi\alpha}+1)\zeta(\alpha-1)y^\alpha}}. \tag{C20}$$

The previous equation in the limit $y \to 0$ gives

$$\mathrm{Im}\,R_0(iy) = \begin{cases} y^{1-\alpha} & \text{for } \alpha < 1, \\ y^{2\alpha-2} & \text{for } 1 < \alpha < 2, \\ y^\alpha & \text{for } \alpha > 2 \end{cases} \tag{C21}$$

and, after performing the last integral in Eq. (C18), the asymptotic behavior of C_0 turns out to be

$$C_0(\ell) \sim \begin{cases} 1/\ell^{2-\alpha} & \text{for } \alpha < 1, \\ 1/\ell^{2\alpha-1} & \text{for } 1 < \alpha < 2, \\ 1/\ell^{\alpha+1} & \text{for } \alpha > 2. \end{cases} \tag{C22}$$

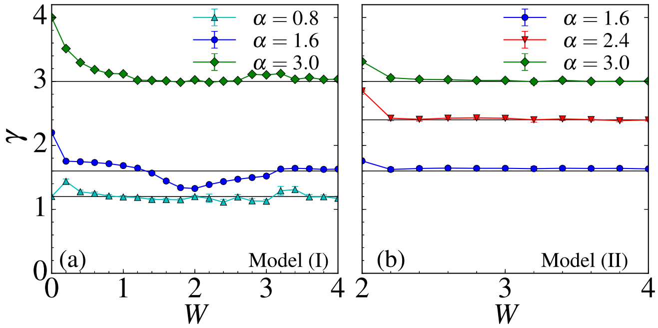

FIG. 8. (a) Decay exponent γ of the long-distance tail of the correlation function $C(\ell)$ for the model I as a function of W and for $\alpha = 0.8$ (cyan triangles), $\alpha = 1.6$ (blue circles), $\alpha = 3.0$ (green diamonds). If $W > 0$, the decay exponent satisfies $\gamma \sim \alpha$ for $\alpha > 1$ and $\gamma \sim 2 - \alpha$ for $\alpha < 1$ and it does not show significance dependence on W. These data are obtained by computing the correlation function $C(\ell)$ numerically from the full random Hamiltonian in Eq. (1) and then by fitting the long-range decaying tail of $C(\ell)$ with $1/\ell^{\gamma}$. The black lines represent the expected exponents: $\gamma = 1.2$ for $\alpha = 0.8$, $\gamma = 1.6$ for $\alpha = 1.6$, $\gamma = 3.0$ for $\alpha = 3.0$. (b) Same as (a) but for the localized phase (for $W \gtrsim 2$) of model II.

For the correlator $C_1(\ell)$ in Eq. (C11) we can use the same contour in Fig. 7 and get

$$C_1(\ell) = \frac{W^2}{3\pi} \int_0^{\infty} dy\, e^{-y\ell}\, \mathrm{Im}\, R_1(iy). \tag{C23}$$

For the asymptotic behavior of $C_1(\ell)$, we need again the $y \to 0$ part of $R_1(iy)$. Let us start by noting that from Eqs. (C14) and (C15) the $y \to 0$ part of both $U(iy)$ and $V(iy)$ is given by

$$\begin{aligned} \mathrm{Im}[U(iy)|u_{iy}|^2] &\sim \mathrm{Im}[V(iy)|v_{iy}|^2] \\ &\sim \mathrm{Im}\, \frac{f_\alpha(iy)(\mu - \cosh y)}{\lambda_\alpha^2(iy)} \\ &\sim \begin{cases} y^{1-\alpha} & \text{for } \alpha < 1, \\ y^{\alpha-1} & \text{for } \alpha > 1. \end{cases} \end{aligned} \tag{C24}$$

The previous equation, by considering also the contribution coming from $c|u_{iy}|^2$ [see Eq. (C12)], gives

$$\mathrm{Im}\, R_1(iy) \sim \begin{cases} y^{1-\alpha} & \text{for } \alpha < 1, \\ y^{\alpha-1} & \text{for } \alpha > 1 \end{cases} \tag{C25}$$

and after integrating Eq. (C23), we finally get the correlator

$$C_1(\ell) = \begin{cases} W^2/\ell^{2-\alpha} & \text{for } \alpha < 1, \\ W^2/\ell^{\alpha} & \text{for } \alpha > 1. \end{cases} \tag{C26}$$

The asymptotic behavior coming from Eqs. (C22) and (C26) can be checked by computing the correlator $C(\ell)$ numerically as reported in Fig. 2(a) of the main text. Remarkably, the values of the decay exponents of the power-law tails do not depend on the disorder strength W as shown in Fig. 8 where we plot the decay exponents of $C(\ell)$ as a function of W for different values of α. For completeness, we show also the decay exponent of the correlation function $C(\ell)$ for the model II with random long-range pairing.

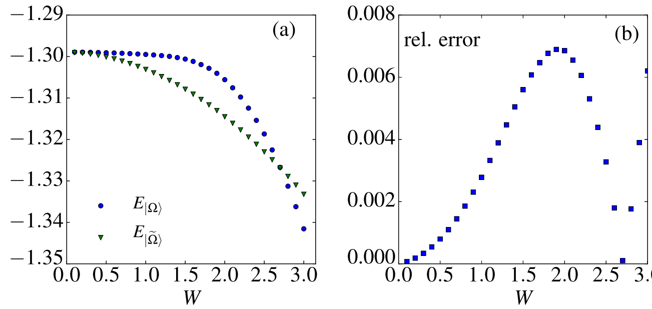

FIG. 9. (a) Energy density $E_{|\Omega\rangle}/L$ of the ground state of the Hamiltonian H_{I} computed numerically (blue circles) and the energy $E_{|\widetilde{\Omega}_0\rangle}/L$ (green triangles) computed by perturbation theory. (b) Relative error defined as $|1 - E_{|\widetilde{\Omega}\rangle}/E_{|\Omega\rangle}|$. It is possible to see that the difference between the true ground-state energy and the perturbed one is bounded by $8 \times\ 10^{-3}$ when the disorder strength satisfies $0 \leqslant W \leqslant 3$. For both panels we consider $\alpha = 3.0$ and a system of $L = 400$ sites and after averaging 200 disorder realizations.

3. Validity of the perturbation theory

In this section we give some details on the validity of the perturbation theory in approximating the true ground state of H_{I} by the state $|\widetilde{\Omega}\rangle$ in Eq. (C7). To this end, we will compare the energy $E_{|\Omega\rangle}$ of the ground state of the Hamiltonian H_{I} computed numerically with the energy $E_{|\widetilde{\Omega}\rangle}$ of the state $|\widetilde{\Omega}\rangle = |\Omega_0\rangle + |\delta\Omega_0\rangle$ coming from the first-order correction given in Eq. (C7).

The energy $E_{|\widetilde{\Omega}\rangle}$ can be obtained by considering that the first-order correction to a wave function gives a second-order correction to the energy [135]. Therefore, the energy for the perturbed state $|\widetilde{\Omega}\rangle$ is given by

$$E_{|\widetilde{\Omega}\rangle} = E_{|\Omega_0\rangle} + \sum_{\mathbf{n}_0} \frac{|\langle \Omega_0 | V_{\mathrm{I}} | \mathbf{n}_0 \rangle|^2}{E_{|\Omega_0\rangle} - E_{|\mathbf{n}_0\rangle}}, \tag{C27}$$

where $E_{|\Omega_0\rangle}$ is the ground-state energy of the Hamiltonian H_0, $|\mathbf{n}_0\rangle$ denotes the excited states of H_0 from Eq. (C6), and $E_{|\mathbf{n}_0\rangle}$ denotes their energy.

By computing the scalar product $\langle \mathbf{n}_0 | V_{\mathrm{I}} | \Omega_0 \rangle$ we get

$$E_{|\widetilde{\Omega}\rangle} = E_{|\Omega_0\rangle} - \sum_{q_1,q_2} \frac{|\mathcal{E}_{q_1,q_2}|^2}{\lambda_\alpha(q_1) + \lambda_\alpha(q_2)}, \tag{C28}$$

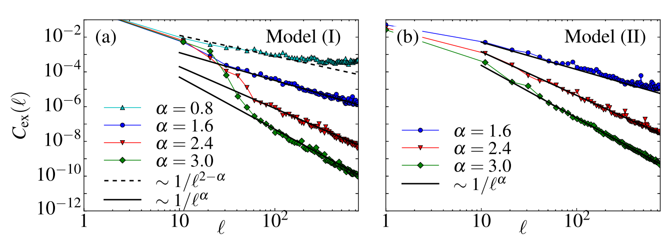

FIG. 10. Correlation function $C_{\mathrm{ex}}(\ell)$ computed on an excited state at the middle of the energy band for the model I as a function of the lattice site ℓ for different values of α and for $W = 5$, $L = 1000$ and 200 disorder realizations. The continuous lines are guides to the eye and show that the power-law tails scale as $1/\ell^{2-\alpha}$ (dashed) and $1/\ell^{2\alpha}$ (solid) also for that excited state. (b) Same as (a) but for the model II.

where $\mathcal{E}_{q_1,q_2} = 2J_{q_1,q_2} e^{iq_1} v_{q_1} u^*_{q_2}$ + H.c. where v_{q_1} and u_{q_2} are defined after Eq. (C5) and J_{q_1,q_2} after Eq. (C7). The left panel of Fig. 9 shows the values of the energy density $E_{|\Omega\rangle}/L$ of the ground state of the Hamiltonian $H_{\rm I}$ computed numerically (blue circles) with the energy $E_{|\widetilde{\Omega}_0\rangle}/L$ (green triangles), while the right panel shows the relative error defined as $|1 - E_{|\widetilde{\Omega}\rangle}/E_{|\Omega\rangle}|$ for a system of $L = 400$ sites and after averaging 200 disorder realizations for $\alpha = 3.0$. It is possible to see that the difference between the true ground-state energy and the perturbed one is bounded by 8×10^{-3} when the disorder strength satisfies $0 \leqslant W \leqslant 3$.

4. Correlators on excited states

In order to show that the algebraic tail of the correlators $a^\dagger_j a_\ell$ is not peculiar only to the ground state, but it is typical also for the excited states, we computed the correlation $C_{\rm ex}(j,\ell) = \langle\Omega|\eta_q\, a^\dagger_j a_\ell\, \eta^\dagger_q|\Omega\rangle$ for the excited state $\eta^\dagger_q|\Omega\rangle$. In Fig. 10 we plot $C_{\rm ex}(j,\ell)$ for an excited state that lies in the middle of the energy band for both the models I and II and for different values of α. It is possible to see that the algebraic tail is present also in this case.

[1] P. W. Anderson, Phys. Rev. **109**, 1492 (1958).
[2] G. Roati, C. D'Errico, L. Fallani, M. Fattori, C. Fort, M. Zaccanti, G. Modugno, M. Modugno, and M. Inguscio, Nature (London) **453**, 895 (2008).
[3] J. Billy, V. Josse, Z. Zuo, A. Bernard, B. Hambrecht, P. Lugan, D. Clement, L. Sanchez-Palencia, P. Bouyer, and A. Aspect, Nature (London) **453**, 891 (2008).
[4] S. S. Kondov, W. R. McGehee, J. J. Zirbel, and B. DeMarco, Science **334**, 66 (2011).
[5] F. Jendrzejewski, A. Bernard, K. Muller, P. Cheinet, V. Josse, M. Piraud, L. Pezze, L. Sanchez-Palencia, A. Aspect, and P. Bouyer, Nat. Phys. **8**, 398 (2012).
[6] M. Schreiber, S. S. Hodgman, P. Bordia, H. P. Lüschen, M. H. Fischer, R. Vosk, E. Altman, U. Schneider, and I. Bloch, Science **349**, 842 (2015).
[7] J. Smith, A. Lee, P. Richerme, B. Neyenhuis, P. W. Hess, P. Hauke, M. Heyl, D. A. Huse, and C. Monroe, Nat. Phys. **12**, 907 (2016).
[8] P. Bordia, H. P. Lüschen, S. S. Hodgman, M. Schreiber, I. Bloch, and U. Schneider, Phys. Rev. Lett. **116**, 140401 (2016).
[9] P. A. Lee and T. V. Ramakrishnan, Rev. Mod. Phys. **57**, 287 (1985).
[10] B. L. Altshuler, Y. Gefen, A. Kamenev, and L. S. Levitov, Phys. Rev. Lett. **78**, 2803 (1997).
[11] D. Basko, I. Aleiner, and B. Altshuler, Ann. Phys. **321**, 1126 (2006).
[12] V. Oganesyan and D. A. Huse, Phys. Rev. B **75**, 155111 (2007).
[13] I. V. Gornyi, A. D. Mirlin, and D. G. Polyakov, Phys. Rev. Lett. **95**, 206603 (2005).
[14] M. Žnidarič, T. Prosen, and P. Prelovšek, Phys. Rev. B **77**, 064426 (2008).
[15] J. Biddle, B. Wang, D. J. Priour, Jr., and S. Das Sarma, Phys. Rev. A **80**, 021603(R) (2009).
[16] J. Biddle and S. Das Sarma, Phys. Rev. Lett. **104**, 070601 (2010).
[17] J. Biddle, D. J. Priour, B. Wang, and S. Das Sarma, Phys. Rev. B **83**, 075105 (2011).
[18] A. Pal and D. A. Huse, Phys. Rev. B **82**, 174411 (2010).
[19] A. D. Luca and A. Scardicchio, Europhys. Lett. **101**, 37003 (2013).
[20] R. Vosk and E. Altman, Phys. Rev. Lett. **110**, 067204 (2013).
[21] Y. Bar Lev and D. R. Reichman, Phys. Rev. B **89**, 220201(R) (2014).
[22] Y. Bar Lev, G. Cohen, and D. R. Reichman, Phys. Rev. Lett. **114**, 100601 (2015).
[23] D. J. Luitz, N. Laflorencie, and F. Alet, Phys. Rev. B **91**, 081103(R) (2015).
[24] D. J. Luitz, Phys. Rev. B **93**, 134201 (2016).
[25] P. Naldesi, E. Ercolessi, and T. Roscilde, Sci. Post. Phys. **1**, 010 (2016).
[26] R. Nandkishore, S. Gopalakrishnan, and D. A. Huse, Phys. Rev. B **90**, 064203 (2014).
[27] I. V. Gornyi, A. D. Mirlin, M. Müller, and D. G. Polyakov, Ann. Phys. **529**, 1600365 (2017).
[28] A. C. Potter and R. Vasseur, Phys. Rev. B **94**, 224206 (2016).
[29] J. T. Cantin, T. Xu, and R. V. Krems, Phys. Rev. B **98**, 014204 (2018).
[30] D. J. Luitz and Y. B. Lev, Phys. Rev. A **99**, 010105(R) (2019).
[31] X.-L. Deng, D. Porras, and J. I. Cirac, Phys. Rev. A **72**, 063407 (2005).
[32] M. Kastner, Phys. Rev. Lett. **104**, 240403 (2010).
[33] Z.-X. Gong, M. Foss-Feig, S. Michalakis, and A. V. Gorshkov, Phys. Rev. Lett. **113**, 030602 (2014).
[34] M. Foss-Feig, Z.-X. Gong, C. W. Clark, and A. V. Gorshkov, Phys. Rev. Lett. **114**, 157201 (2015).
[35] P. Hauke and L. Tagliacozzo, Phys. Rev. Lett. **111**, 207202 (2013).
[36] J. Eisert, M. van den Worm, S. R. Manmana, and M. Kastner, Phys. Rev. Lett. **111**, 260401 (2013).
[37] J. Schachenmayer, B. P. Lanyon, C. F. Roos, and A. J. Daley, Phys. Rev. X **3**, 031015 (2013).
[38] D. Métivier, R. Bachelard, and M. Kastner, Phys. Rev. Lett. **112**, 210601 (2014).
[39] M. Kastner and M. van den Worm, Phys. Scr. **2015**, 014039 (2015).
[40] L. Cevolani, G. Carleo, and L. Sanchez-Palencia, Phys. Rev. A **92**, 041603(R) (2015).
[41] L. Cevolani, G. Carleo, and L. Sanchez-Palencia, New J. Phys. **18**, 093002 (2016).
[42] R. J. Bettles, J. Minář, C. S. Adams, I. Lesanovsky, and B. Olmos, Phys. Rev. A **96**, 041603(R) (2017).
[43] S. Hernández-Santana, C. Gogolin, J. I. Cirac, and A. Acín, Phys. Rev. Lett. **119**, 110601 (2017).
[44] I. Frérot, P. Naldesi, and T. Roscilde, Phys. Rev. B **95**, 245111 (2017).
[45] I. Frérot, P. Naldesi, and T. Roscilde, Phys. Rev. Lett. **120**, 050401 (2018).
[46] C. Schneider, D. Porras, and T. Schätz, Rep. Prog. Phys. **75**, 024401 (2012).

[47] P. Richerme, Z.-X. Gong, A. Lee, C. Senko, J. Smith, M. Foss-Feig, S. Michalakis, A. V. Gorshkov, and C. Monroe, Nature (London) **511**, 198 (2014).
[48] P. Jurcevic, B. P. Lanyon, P. Hauke, C. Hempel, P. Zoller, R. Blatt, and C. F. Roos, Nature (London) **511**, 202 (2014).
[49] J. W. Britton, B. C. Sawyer, A. C. Keith, C. C. J. Wang, J. K. Freericks, H. Uys, M. J. Biercuk, and J. J. Bollinger, Nature (London) **484**, 489 (2012).
[50] A. Bermudez, T. Schäetz, and M. B. Plenio, Phys. Rev. Lett. **110**, 110502 (2013).
[51] E. Shahmoon and G. Kurizki, Phys. Rev. A **87**, 033831 (2013).
[52] J. S. Douglas, H. Habibian, C. L. Hung, A. V. Gorshkov, H. J. Kimble, and D. E. Chang, Nat. Photonics **9**, 326 (2015).
[53] M. Litinskaya, E. Tignone, and G. Pupillo, Sci. Rep. **6**, 25630 (2016).
[54] V. D. Vaidya, Y. Guo, R. M. Kroeze, K. E. Ballantine, A. J. Kollár, J. Keeling, and B. L. Lev, Phys. Rev. X **8**, 011002 (2018).
[55] H. Kadau, M. Schmitt, M. Wenzel, C. Wink, T. Maier, I. Ferrier-Barbut, and T. Pfau, Nature (London) **530**, 194 (2016).
[56] S. Lepoutre, L. Gabardos, K. Kechadi, P. Pedri, O. Gorceix, E. Maréchal, L. Vernac, and B. Laburthe-Tolra, Phys. Rev. Lett. **121**, 013201 (2018).
[57] S. Baier, D. Petter, J. H. Becher, A. Patscheider, G. Natale, L. Chomaz, M. J. Mark, and F. Ferlaino, Phys. Rev. Lett. **121**, 093602 (2018).
[58] Y. Tang, W. Kao, K.-Y. Li, and B. L. Lev, Phys. Rev. Lett. **120**, 230401 (2018).
[59] H. Weimer, R. Löw, T. Pfau, and H. P. Büchler, Phys. Rev. Lett. **101**, 250601 (2008).
[60] M. Saffman, T. G. Walker, and K. Mølmer, Rev. Mod. Phys. **82**, 2313 (2010).
[61] M. Viteau, P. Huillery, M. G. Bason, N. Malossi, D. Ciampini, O. Morsch, E. Arimondo, D. Comparat, and P. Pillet, Phys. Rev. Lett. **109**, 053002 (2012).
[62] P. Schauß, M. Cheneau, M. Endres, T. Fukuhara, S. Hild, A. Omran, T. Pohl, C. Gross, S. Kuhr, and I. Bloch, Nature (London) **491**, 87 (2012).
[63] C. Carr, R. Ritter, C. G. Wade, C. S. Adams, and K. J. Weatherill, Phys. Rev. Lett. **111**, 113901 (2013).
[64] D. Barredo, S. Ravets, H. Labuhn, L. Béguin, A. Vernier, F. Nogrette, T. Lahaye, and A. Browaeys, Phys. Rev. Lett. **112**, 183002 (2014).
[65] J. B. Balewski, A. T. Krupp, A. Gaj, S. Hofferberth, R. Löw, and T. Pfau, New J. Phys. **16**, 063012 (2014).
[66] Y. Y. Jau, A. M. Hankin, T. Keating, I. H. Deutsch, and G. W. Biedermann, Nat. Phys. **12**, 71 (2015).
[67] T. M. Weber, M. Höning, T. Niederprüm, T. Manthey, O. Thomas, V. Guarrera, M. Fleischhauer, G. Barontini, and H. Ott, Nat. Phys. **11**, 157 (2015).
[68] R. Faoro, C. Simonelli, M. Archimi, G. Masella, M. M. Valado, E. Arimondo, R. Mannella, D. Ciampini, and O. Morsch, Phys. Rev. A **93**, 030701(R) (2016).
[69] H. Labuhn, D. Barredo, S. Ravets, S. de Léséleuc, T. Macrì, T. Lahaye, and A. Browaeys, Nature (London) **534**, 667 (2016).
[70] H. Gorniaczyk, C. Tresp, P. Bienias, A. Paris-Mandoki, W. Li, I. Mirgorodskiy, H. P. Büchler, I. Lesanovsky, and S. Hofferberth, Nat. Commun. **7**, 12480 (2016).
[71] J. Zeiher, R. van Bijnen, P. Schauß, S. Hild, J.-y. Choi, T. Pohl, I. Bloch, and C. Gross, Nat. Phys. **12**, 1095 (2016).
[72] H. Bernien, S. Schwartz, A. Keesling, H. Levine, A. Omran, H. Pichler, S. Choi, A. S. Zibrov, M. Endres, M. Greiner, V. Vuletić, and M. D. Lukin, Nature (London) **551**, 579 (2017).
[73] A. Piñeiro Orioli, A. Signoles, H. Wildhagen, G. Günter, J. Berges, S. Whitlock, and M. Weidemüller, Phys. Rev. Lett. **120**, 063601 (2018).
[74] B. Yan, S. A. Moses, B. Gadway, J. P. Covey, K. R. A. Hazzard, A. M. Rey, D. S. Jin, and J. Ye, Nature (London) **501**, 521 (2013).
[75] K. R. A. Hazzard, M. van den Worm, M. Foss-Feig, S. R. Manmana, E. G. Dalla Torre, T. Pfau, M. Kastner, and A. M. Rey, Phys. Rev. A **90**, 063622 (2014).
[76] L. Reichsöllner, A. Schindewolf, T. Takekoshi, R. Grimm, and H.-C. Nägerl, Phys. Rev. Lett. **118**, 073201 (2017).
[77] G. A. Álvarez, D. Suter, and R. Kaiser, Science **349**, 846 (2015).
[78] W. R. Anderson, J. R. Veale, and T. F. Gallagher, Phys. Rev. Lett. **80**, 249 (1998).
[79] W. R. Anderson, M. P. Robinson, J. D. D. Martin, and T. F. Gallagher, Phys. Rev. A. **65**, 063404 (2002).
[80] G. D. Scholes and G. Rumbles, Nat. Mater. **5**, 683 (2006).
[81] F. Dubin, R. Melet, T. Barisien, R. Grousson, L. Legrand, M. Schott, and V. Voliotis, Nat. Phys. **2**, 32 (2005).
[82] F. Dubin, J. Berréhar, R. Grousson, M. Schott, and V. Voliotis, Phys. Rev. B **73**, 121302(R) (2006).
[83] X. P. Vögele, D. Schuh, W. Wegscheider, J. P. Kotthaus, and A. W. Holleitner, Phys. Rev. Lett. **103**, 126402 (2009).
[84] S. Wüster, C. Ates, A. Eisfeld, and J. M. Rost, New J. Phys. **13**, 073044 (2011).
[85] G. Günter, H. Schempp, M. Robert-de Saint-Vincent, V. Gavryusev, S. Helmrich, C. S. Hofmann, S. Whitlock, and M. Weidemüller, Science **342**, 954 (2013).
[86] F. Robicheaux and N. M. Gill, Phys. Rev. A **89**, 053429 (2014).
[87] D. W. Schönleber, A. Eisfeld, M. Genkin, S. Whitlock, and S. Wüster, Phys. Rev. Lett. **114**, 123005 (2015).
[88] H. Schempp, G. Günter, S. Wüster, M. Weidemüller, and S. Whitlock, Phys. Rev. Lett. **115**, 093002 (2015).
[89] D. Barredo, H. Labuhn, S. Ravets, T. Lahaye, A. Browaeys, and C. S. Adams, Phys. Rev. Lett. **114**, 113002 (2015).
[90] I. Rosenberg, D. Liran, Y. Mazuz-Harpaz, K. West, L. Pfeiffer, and R. Rapaport, Sci. Adv. **4**, eaat8880 (2018).
[91] F. Pientka, L. I. Glazman, and F. von Oppen, Phys. Rev. B **88**, 155420 (2013).
[92] F. Pientka, L. I. Glazman, and F. von Oppen, Phys. Rev. B **89**, 180505(R) (2014).
[93] D. T. Liu, J. Shabani, and A. Mitra, Phys. Rev. B **97**, 235114 (2018).
[94] D. T. Liu, J. Shabani, and A. Mitra, Phys. Rev. B **99**, 094303 (2019).
[95] A. Y. Kitaev, Phys. Usp. **44**, 131 (2001).
[96] F. Liu, R. Lundgren, P. Titum, G. Pagano, J. Zhang, C. Monroe, and A. V. Gorshkov, Phys. Rev. Lett. **122**, 150601 (2019).
[97] J. Zhang, P. W. Hess, A. Kyprianidis, P. Becker, A. Lee, J. Smith, G. Pagano, I. D. Potirniche, A. C. Potter, A. Vishwanath, N. Y. Yao, and C. Monroe, Nature (London) **543**, 217 (2017).
[98] O. Viyuela, D. Vodola, G. Pupillo, and M. A. Martin-Delgado, Phys. Rev. B **94**, 125121 (2016).

[99] Z.-X. Gong, M. F. Maghrebi, A. Hu, M. L. Wall, M. Foss-Feig, and A. V. Gorshkov, Phys. Rev. B **93**, 041102(R) (2016).
[100] L. Lepori and L. Dell'Anna, New J. Phys. **19**, 103030 (2017).
[101] K. Patrick, T. Neupert, and J. K. Pachos, Phys. Rev. Lett. **118**, 267002 (2017).
[102] O. Viyuela, L. Fu, and M. A. Martin-Delgado, Phys. Rev. Lett. **120**, 017001 (2018).
[103] L. Lepori, D. Giuliano, and S. Paganelli, Phys. Rev. B **97**, 041109(R) (2018).
[104] D. Vodola, L. Lepori, E. Ercolessi, A. V. Gorshkov, and G. Pupillo, Phys. Rev. Lett. **113**, 156402 (2014).
[105] F. Ares, J. G. Esteve, F. Falceto, and A. R. de Queiroz, Phys. Rev. A **92**, 042334 (2015).
[106] Z.-X. Gong, M. Foss-Feig, F. G. S. L. Brandão, and A. V. Gorshkov, Phys. Rev. Lett. **119**, 050501 (2017).
[107] N. Roy, A. Sharma, and R. Mukherjee, Phys. Rev. A **99**, 052342 (2019).
[108] L. S. Levitov, Europhys.s Letters **9**, 83 (1989).
[109] L. S. Levitov, Phys. Rev. Lett. **64**, 547 (1990).
[110] A. D. Mirlin, Y. V. Fyodorov, F.-M. Dittes, J. Quezada, and T. H. Seligman, Phys. Rev. E **54**, 3221 (1996).
[111] A. Rodríguez, V. A. Malyshev, and F. Domínguez-Adame, J. Phys. A: Math. Gen. **33**, L161 (2000).
[112] A. Rodríguez, V. A. Malyshev, G. Sierra, M. A. Martín-Delgado, J. Rodríguez-Laguna, and F. Domínguez-Adame, Phys. Rev. Lett. **90**, 027404 (2003).
[113] F. A. B. F. de Moura, A. V. Malyshev, M. L. Lyra, V. A. Malyshev, and F. Domínguez-Adame, Phys. Rev. B **71**, 174203 (2005).
[114] G. L. Celardo, R. Kaiser, and F. Borgonovi, Phys. Rev. B **94**, 144206 (2016).
[115] X. Deng, V. E. Kravtsov, G. V. Shlyapnikov, and L. Santos, Phys. Rev. Lett. **120**, 110602 (2018).
[116] D. Vodola, L. Lepori, E. Ercolessi, and G. Pupillo, New J. Phys. **18**, 015001 (2016).
[117] T. Koffel, M. Lewenstein, and L. Tagliacozzo, Phys. Rev. Lett. **109**, 267203 (2012).
[118] A. L. Burin, Phys. Rev. B **91**, 094202 (2015).
[119] E. Lieb, T. Schultz, and D. Mattis, Ann. Phys. (NY) **16**, 407 (1961).
[120] P. Hauke and M. Heyl, Phys. Rev. B **92**, 134204 (2015).
[121] H. Li, J. Wang, X.-J. Liu, and H. Hu, Phys. Rev. A **94**, 063625 (2016).
[122] A. O. Maksymov, N. Rahman, E. Kapit, and A. L. Burin, Phys. Rev. A **96**, 057601 (2017).
[123] C. L. Baldwin, C. R. Laumann, A. Pal, and A. Scardicchio, Phys. Rev. Lett. **118**, 127201 (2017).
[124] D. A. Abanin and Z. Papić, Ann. Phys. **529**, 1700169 (2017).
[125] L. Lepori, D. Vodola, G. Pupillo, G. Gori, and A. Trombettoni, Ann. Phys. **374**, 35 (2016).
[126] M. F. Maghrebi, Z.-X. Gong, M. Foss-Feig, and A. V. Gorshkov, Phys. Rev. B **93**, 125128 (2016).
[127] L. Lepori, A. Trombettoni, and D. Vodola, J. Stat. Mech.: Theory Exp. (2017) 033102.
[128] S. R. White, Phys. Rev. Lett. **69**, 2863 (1992).
[129] http://itensor.org/.
[130] J. J. Sakurai and J. Napolitano, *Modern Quantum Mechanics*, 2nd ed. (Addison-Wesley, Boston, 2011).
[131] A. Altland and B. Simons, *Condensed Matter Field Theory* (Cambridge University Press, Cambridge, England, 2006).
[132] H. Bruus and K. Flensberg, *Many-Body Quantum Theory in Condensed Matter Physics: An Introduction* (Oxford University Press, Oxford, 2004).
[133] M. Abramowitz and I. A. Stegun, *Handbook of Mathematical Functions* (Dover, New York, 1964).
[134] F. W. J. Olver, D. W. Lozier, R. F. Boisvert, and C. W. Clark, *NIST Handbook of Mathematical Functions* (Cambridge University Press, Cambridge, England, 2010).
[135] K. Gottfried and T.-M. Yan, *Quantum Mechanics: Fundamentals* (Springer, Berlin, 2003).